

# The spectral and magnetic properties of $\alpha$ - and $\gamma$ -Ce from the Dynamical Mean-Field Theory and Local Density Approximation

M.B. Zöhl<sup>1</sup>, I.A. Nekrasov<sup>2</sup>, Th. Pruschke<sup>1</sup>, V.I. Anisimov<sup>2</sup>, and J. Keller<sup>1</sup>

<sup>1</sup>*Institut für Theoretische Physik I, Universität Regensburg, Universitätsstr. 31, 93053 Regensburg, Germany*

<sup>2</sup>*Institute for Metal Physics, 620219 Yekaterinburg GSP-170, Russia*

(November 1, 2018)

We have calculated ground state properties and excitation spectra for Ce metal with the *ab initio* computational scheme combining local density approximation and dynamical mean-field theory (LDA+DMFT). We considered all electronic states, i.e. correlated *f*-states and non-correlated *s*-, *p*- and *d*-states. The strong local correlations (Coulomb interaction) among the *f*-states lead to typical many-body resonances in the partial *f*-density, such as lower and upper Hubbard band. Additionally the well known Kondo resonance is observed. The *s*-, *p*- and *d*-densities show small to mediate renormalization effects due to hybridization. We observe different Kondo temperatures for  $\alpha$ - and  $\gamma$ -Ce ( $T_{K,\alpha} \approx 1000$  K and  $T_{K,\gamma} \approx 30$  K), due to strong volume dependence of the effective hybridization strength for the localized *f*-electrons. Finally we compare our results with a variety of experimental data, i.e. from photoemission spectroscopy (PES), inverse photoemission spectroscopy (BIS), resonant inverse photoemission spectroscopy (RIPES) and magnetic susceptibility measurements.

71.27.+a Strongly correlated electron systems , 74.25.Jb Electronic structure

Ce metal is the simplest lanthanide compound with only one atom in a face centered cubic (fcc) crystal structure and a relatively small set of relevant electronic states derived from *s*-, *p*- *d*- and *f*-orbitals of Ce. It shows an unique isostructural (fcc to fcc)  $\alpha \rightarrow \gamma$  phase transition with increasing temperature. The high-temperature  $\gamma$  phase has 15% larger volume and displays a Curie-Weiss-like temperature dependence of the magnetic susceptibility signaling the existence of local magnetic moments while the  $\alpha$ -phase has a Pauli-like temperature independent paramagnetism [1].

While many different models were proposed to describe this system (for a review see [2]), the most relevant seems to be the periodic Anderson model. Studies based on the single impurity Anderson model [3] with a hybridization function obtained from LDA band structure calculations were rather successful in reproducing Kondo scales and spectra for  $\alpha$ - and  $\gamma$ -Ce. However, an empirical renormalization of the hybridization function and position of the impurity level were needed for satisfactory agreement between calculated and experimental spectra.

Due to the recent development of the Dynamical Mean-Field Theory [4] a more realistic treatment of Ce is now possible. In contrast to the Hubbard model (degenerate and non-degenerate), where hybridization occurs only between correlated *d*- or *f*-orbitals, Ce is much more complicated. The direct *f*-*f* hybridization is of the same order of magnitude as the hybridization of *f*-orbitals with the delocalized *spd*-states. Thus in order to describe Ce one even has to go beyond the periodic Anderson model, where only hybridization of the correlated *f*-orbitals with the delocalized states is included. In order to address this problem we used the most general procedure for calculating the Green function using a full basis set (*s*, *p*, *d*, *f*) Hamiltonian with the integration over Brillouin zone in *k*-space.

Recently a LDA+DMFT approach was proposed, with different methods to solve the DMFT equations: IPT [5–7], NCA [8,9] and QMC [10–12]. All these three methods were used to investigate  $\text{La}_{1-x}\text{Sr}_x\text{TiO}_3$  [5,8,10]. The same strategy was formulated by Lichtenstein and Katsnelson [7] as one of their LDA++ approaches. Lichtenstein and Katsnelson applied LDA+DMFT(IPT) [13], and were the first to use LDA+DMFT(QMC) [14] to investigate the spectral properties of iron. Liebsch and Lichtenstein also applied LDA+DMFT(QMC) to calculate the photoemission spectrum of  $\text{Sr}_2\text{RuO}_4$  [15].

Here we present results obtained within LDA+DMFT(NCA) [8,9]. After convergence of the DMFT selfconsistent loop the hybridization function corresponds to fully interacting effective medium for the *f*-shell of a Ce ion. The interacting Green function obtained in our calculation allows us to compute ground state properties like orbital occupation values, Kondo temperatures  $T_K$ , magnetic susceptibility  $\chi(0)$ , as well as excitation spectra. Our results show a satisfactory agreement with the experimental data without using any adjustable parameters.

In the following we will concentrate on a simplified local interaction. Here, we introduce two distinct Coulomb parameters: the intra-orbital Coulomb energy  $U$  has to be considered in case of a doubly occupied orbital, while the inter-orbital Coulomb energy  $U'$  applies for example in the case of a doubly occupied *f*-shell with electrons on *f*-orbitals with different indices. Since we neglect any exchange correlations, which is typically of the order of one tenth of the Coulomb interaction, we chose  $U = U'$  in order to fulfill the condition of rotational invariance of the local interaction [16]. A more sophisticated interaction term has been already investigated within the framework of

LDA+DMFT(NCA) scheme [8]. We thus arrive at an interaction of the form

$$H_{corr}^{local} = U \sum_m \hat{n}_{m\uparrow} \hat{n}_{m\downarrow} + \frac{U'}{2} \sum_{m,m',\sigma,\sigma'}^{m \neq m'} \hat{n}_{m\sigma} \hat{n}_{m'\sigma'}. \quad (1)$$

The most important feature of the DMFT is that the proper one-particle selfenergy due to the local Coulomb interaction is purely local [4]. Thus, we obtain as an expression for the full Green function of the interacting system

$$G(z) = \frac{1}{N_{\vec{k}}} \sum_{\vec{k}} (z \overset{\leftrightarrow}{\mathbb{I}} - \overset{\leftrightarrow}{h}(\vec{k}) - \Sigma(z) \overset{\leftrightarrow}{\mathbb{I}}_f)^{-1}, \quad (2)$$

noninteracting one-particle hamiltonian  $\overset{\leftrightarrow}{h}(\vec{k})$  and consequently  $G(z)$  will in general be matrices in orbital space,  $\overset{\leftrightarrow}{\mathbb{I}}_f$  is the diagonal matrix with matrix elements equal 1 for  $f$ -orbitals and zero for all others,  $\overset{\leftrightarrow}{\mathbb{I}}$  is unit matrix. The  $\vec{k}$ -summation is done by a standard tetrahedron method [5]. Within this method one can easily treat hybridization effects between correlated and non-correlated states.

As starting point of our calculation we determined the one particle LDA Hamiltonian with the LMTO method [17] considering the  $6s, 6p, 5d$  and  $4f$ -shells. The noninteracting one-particle hamiltonian  $\overset{\leftrightarrow}{h}(\vec{k})$  was obtained by subtracting the Hartree contribution of (1) from the LDA results in order to avoid double counting [5,8,10]. The value of the Coulomb interaction was calculated by a supercell method [18] and found to be  $U \approx 6$  eV. The chemical potential was adjusted to conserve the number of particles (4 electrons per site) during the selfconsistent LDA+DMFT calculation. Analyzing the partial densities of states one can observe for both  $\alpha$ - and  $\gamma$ -Ce at a temperature of  $T = 580$  K intermediate size renormalization effects, in particular broadening and shifts of structures, for  $s$ - and  $d$ -states and only marginal effects for the  $p$ -states. This is a consequence of hybridization, which is seen by a non-vanishing  $s$ - or  $d$ -density at the position of the  $f$ -states in the LDA result. The  $f$ -states are strongly renormalized. A lower Hubbard band (LHB) is observed at the position of the corrected (double counting) LDA  $f$ -state (at about  $-3$  eV). The upper Hubbard band (UHB) is situated at about 4.5 eV and describes an excitation of a doubly occupied  $f$ -state. At the Fermi level one observes a Kondo resonance (KR) for  $\alpha$ -Ce, which can be described by a singlet formation between an unpaired  $f$ -electron and the surrounding conduction electrons. The  $d$ -density for  $\alpha$ -Ce shows an onset of a hybridization gap, which is well known in model calculations for the periodic Anderson model [19] and is a consequence of the formation of the singlet state between the unpaired  $f$ -spins and the conduction electrons. For  $\gamma$ -Ce one observes only the onset of a KR as a consequence of the smaller  $T_K$  compared to the  $\alpha$ -phase and thus no hybridization gap opens in the conduction electron density.

In Table I we show a comparison of our results with the results of spectral fits to electron [3] and high-energy neutron spectroscopy [20]. The occupation probabilities are in very good agreement with the experiment, as well as the number of occupied  $f$ -states per site,  $n_f$ . The occupation probabilities  $P_0$ ,  $P_1$  and  $P_2$  for the states  $f^0$ ,  $f^1$  and  $f^2$  were calculated from the particular ionic propagators. The Kondo temperature for  $\alpha$ -Ce  $T_{K,\alpha} \approx 1000$  K is roughly given by the width of the KR. Since for  $\gamma$ -Ce the Abrikosov-Suhl resonance is not yet well developed, it makes no sense to estimate  $T_K$  from the width. Instead, for  $\gamma$ -Ce we estimate the  $T_K$  from the ratio of the hybridization strength at the Fermi level of both considered materials ( $\Im\{\Delta_\alpha(\varepsilon_F)\}/\Im\{\Delta_\gamma(\varepsilon_F)\} = 2$ ). With this relation we obtain  $T_{K,\gamma} \approx \frac{1}{30} T_{K,\alpha}$  [21]. Since the NCA for multi-band models typically underestimates  $T_K$ , it is obvious, that our absolute values cannot be expected to match with the experiments. Nevertheless, the ratio of the Kondo temperatures for the two different phases should be meaningful and are in good agreement to the experiment (see Table I). The static susceptibilities  $\chi(0)$  calculated with the  $T_K$  as an input via  $\chi(0) = C \frac{1-n(f^0)}{T_K}$ , naturally have the same qualitative character. In this formula  $C$  is the Curie constant for the lowest  $4f$ -state with  $j = \frac{5}{2}$  and  $n(f^0)$  is the occupation of the  $f^0$  states. Again, the ratio of the susceptibilities for the both phases are in good agreement with experiment (see Table I). Also in Table I the parameter  $\Delta_{av}$  represents the averaged value of the imaginary part of the hybridization function  $\Im\{\Delta(\omega)\}$  for an energy interval from  $-3$  eV to 0 eV [22]. It is also in reasonable agreement with experiment.

For  $\alpha$ -Ce the evolution of the KR is clearly observed down to a temperature of  $T = 580$  K, whereas in  $\gamma$ -Ce the evolution of a quasi-particle resonance is strongly suppressed in this temperature regime by a smaller hybridization. Nevertheless by decreasing the temperature down to  $T = 116$  K the onset of the many-body resonance can be observed for  $\gamma$ -Ce, too.

A comparison of the imaginary part of the hybridization function for both phases leads to the result that a strong renormalization takes place in comparison to our pure LDA results, which are in agreement with Ref. [3]. The total weight of this quantity for  $\alpha$ -Ce is twice as high as the one for the  $\gamma$ -phase. Here it turns out that the consideration of all hybridization processes is extremely important in order to get a qualitatively good agreement to experimental

results. If one uses a model with correlated  $f$ -states only, one has to consider one electron per site. This would produce a  $f$ -density with the Fermi energy in between the  $f^1$  and  $f^2$  charge excitation peak, the LHB and UHB respectively. Since the hybridization function is proportional to the density of states one would observe only a small hybridization at the Fermi energy. Thus the additional  $s$ -,  $p$ - and  $d$ -conduction states strongly contribute to the hybridization function at the Fermi energy and lead therefore to different  $T_K$ .

In the PES data for  $\alpha$ -Ce in upper part of Fig. 1 the observed peaks are identified as  $f$ -contributions to the density of states by a cross section argument using different photon energies [23]. Thus we compare the experiment with the calculated partial density for  $f$ -states. The theoretical  $f$ -spectrum shows a LHB which is also seen in the experiment.

The BIS spectrum for  $\alpha$ -Ce shows a main structure between 3 eV and 7 eV, which is attributed to  $4f^2$  final state multiplets. In the calculated spectrum all excitations to  $4f^2$  states are described by the featureless UHB. As a consequence of the simplified interaction model all doubly occupied states are degenerate. This shortcoming in our calculation is responsible for the sharp peaked structure of this feature. The neglected exchange interaction would produce a multiplet structure, which would be closer to the experiment. The experimental peak at about 0.5 eV is attributed to two  $4f^1$  final states, which are split by spin-orbit coupling. The calculated  $f$ -spectrum shows a sharp KR slightly above the Fermi energy, which is the result of the formation of a singlet state between  $f$ - and conduction states. We thus suggest that the spectral weight seen in the experiment is a result of this KR. Since we did not yet include spin-orbit coupling in our model, we of course cannot observe the mentioned splitting of the resonance. However, as it is well known [24], the introduction of such a splitting would eventually split the KR. If we used the experimentally determined value of about 0.3 eV for the spin-orbit splitting [25], the observed resonance of width 0.5 eV would indeed occur in the calculations.

In the lower part of Fig. 1 a comparison between experiment and our calculation for  $\gamma$ -Ce is shown. The most striking difference between lower and upper figures is the absence of the KR in the high temperature phase ( $\gamma$ -Ce; transition temperature 141 K [1]) which is in agreement with our calculations.

In Fig. 2 our results for the non-occupied states in the  $f$ -density are compared with RIPES data [26]. The calculated  $f$ -spectra were multiplied by the Fermi-step function and broadened with an Lorentzian of the width 0.1 eV in order to mimic the experimental resolution in the theoretical curves. Here, as above the theoretical overestimation of the UHB is a consequence of the simplified local interaction and thus of the missing multiplet structure of the  $4f^2$ -final states. The main feature of the experimental spectra: strong decreasing of the intensity ratio for KR and UHB peaks going from  $\alpha$ - to  $\gamma$ -phase, can be also seen for theoretical curves.

In conclusion we have described a realization of a combination of density-functional theory in the local density approximation and the dynamical mean field theory to obtain a first-principles computational scheme for Heavy-Fermion systems. The scheme was set up for the first time with a combination of correlated and non-correlated states in order to introduce the important effect of hybridization between  $s$ -,  $p$ -,  $d$ -states and strongly correlated  $f$ -states. The solution of the DMFT equations was done by using the Non-Crossing approximation. We calculated the one-particle spectra for  $\alpha$ - and  $\gamma$ -Ce and found Kondo temperature values ( $T_{K,\alpha} \approx 1000$  K and  $T_{K,\gamma} \approx 30$  K), which explain the experimental results.

We observe quite reasonable results concerning occupation probabilities  $P_0$ ,  $P_1$ ,  $P_2$  and the number of  $f$ -electrons per site  $n_f$ . The ratio of  $T_K$  and thus the static susceptibilities  $\chi(0)$  values for two phases are in fair agreement with the experimental results considering the problems of the NCA method. Moreover we found qualitative good agreement with PES, BIS and RIPES experiments, i.e. the position of LHB, UHB and the Kondo resonance.

This work was partially supported by the DFG grant PR 298/5-1&2 and Russian Foundation for Basic Research Grant No. RFFI-98-02-17275.

- 
- [1] K.A. Gschneidner, Jr., R.O. Elliott, and R.R. McDonald, J. Phys. Chem. Solids **23**, 1191 (1962); D.C. Koskimaki and K.A. Gschneidner, Jr., Phys. Rev. B **11**, 4463 (1975); J.M. Lawrence and R.D. Parks, J. Phys. (Paris) Colloq. **37**, C4-249 (1976).
  - [2] A. K. McMahan, C. Huscroft, R. T. Scalettar, E. L. Pollock J. Comput.-Aided Mater. Des. **5**, 131 (1998).
  - [3] L.Z. Liu, J.W. Allen, O. Gunnarson, N.E. Christensen, O.K. Andersen, Phys. Rev. B **45**, 8934 (1992).
  - [4] D. Vollhardt in *Correlated Electron Systems*, edited by V. J. Emery, World Scientific, Singapore, 1993, p. 57; Th. Pruschke, M. Jarrell, and J. K. Freericks, Adv. in Phys. **44**, 187 (1995); A. Georges, G. Kotliar, W. Krauth, and M. J. Rozenberg, Rev. Mod. Phys. **68**, 13 (1996).
  - [5] V. I. Anisimov, A. I. Poteryaev, M. A. Korotin, A. O. Anokhin, and G. Kotliar, J. Phys. Cond. Matter **9**, 7359 (1997).

- [6] H. Kajueter and G. Kotliar, *Int. J. Mod. Phys.* **11**, 729 (1997).
- [7] A. I. Lichtenstein and M. I. Katsnelson, *Phys. Rev. B* **57**, 6884 (1998).
- [8] M. B. Zölfw, Th. Pruschke, J. Keller, A. I. Poteryaev, I. A. Nekrasov, and V. I. Anisimov, *Phys. Rev. B* **61**, 12810 (2000).
- [9] H. Keiter, J.C. Kimbal, *Phys. Rev. Lett.* **25**, 672 (1970); N.E. Bickers, D.L. Cox, J.W. Wilkins, *Phys. Rev. B* **36**, 2036 (1987).
- [10] I. A. Nekrasov, K. Held, N. Blümer, A. I. Poteryaev, V. I. Anisimov, and D. Vollhardt, *Euro Phys. J. B* **18**, 55 (2000).
- [11] K. Held, I. A. Nekrasov, N. Blümer, V. I. Anisimov, and D. Vollhardt, preprint cond-mat/0010395.
- [12] M. J. Rozenberg, *Phys. Rev. B* **55**, R4855 (1997); J. E. Han, M. Jarrell, and D. L. Cox, *Phys. Rev. B* **58**, R4199 (1998); K. Held and D. Vollhardt, *Euro. Phys. J. B* **5**, 473 (1998).
- [13] M.I. Katsnelson and A.I. Lichtenstein, *J. Phys. Cond. Matter* **11**, 1037 (1999);
- [14] M.I. Katsnelson and A.I. Lichtenstein, preprint cond-mat/9904428 (1999).
- [15] A. Liebsch and A. Lichtenstein, *Phys. Rev. Lett.* **84**, 1591 (2000).
- [16] K. Held, D. Vollhard, *Euro. Phys. J. B* **5**, 473 (1998).
- [17] O.K. Andersen, *Phys. Rev. B* **12**, 3060 (1975).
- [18] V.I. Anisimov, and O. Gunnarsson, *Phys. Rev. B* **43**, 7570 (1991).
- [19] Th. Pruschke, R. Bulla, M. Jarrell, *Phys. Rev B* **61**, 12799 (2000).
- [20] A.P. Murani, Z.A. Bowden, A.D. Taylor, R. Osborn, W.G. Marshall, *Phys. Rev B* **48**, 13981 (1993).
- [21] E. Müller-Hartmann, *Z. Phys. B: Condens. Matter* **57**, 281 (1984).
- [22] In our approach we use no compensation factor  $\kappa$ , which was used in [3] in order to consider the effect of a self-interaction-correction (SIC).
- [23] D.M. Wieliczka, C.G. Olson, D.W. Lynch, *Phys. Rev. B* **29**, 3028 (1984).
- [24] T. A. Costi, *Phys. Rev. Lett.* **85**, 1504 (2000).
- [25] E. Wuilloud, H.R. Moser, W.D. Schneider, Y. Baer, *Phys. Rev. B* **28**, 7354 (1983).
- [26] M. Grioni, P. Weibel, D. Malterre, Y. Baer, L. Duo, *Phys. Rev. B* **55**, 2056 (1997).

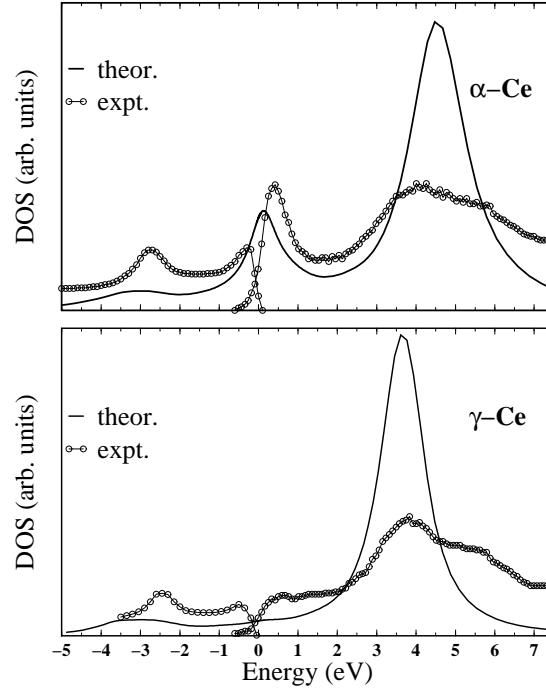


FIG. 1. Comparison between combined PES [23] and BIS [25] experimental (circles) and theoretical (solid line)  $f$ -spectra for  $\alpha$ - (upper part) and  $\gamma$ -Ce (lower part) at  $T = 580$  K. The relative intensities of the BIS and PES portions are roughly for one  $4f$  electron. The experimental and theoretical spectra were normalized and the theoretical curve was broadened with resolution width of  $0.4$  eV.

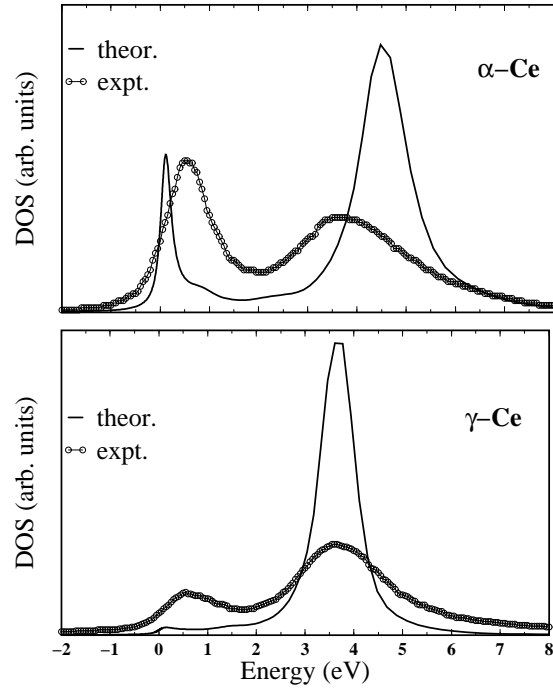


FIG. 2. Comparison between RIPES [26] experimental (circles) and theoretical (solid line)  $f$ -spectra for  $\alpha$ - (upper part) and  $\gamma$ -Ce (lower part) at  $T = 580$  K. The experimental and theoretical were normalized and the theoretical curve was broadened with broadening coefficient of  $0.1$  eV.

TABLE I. Comparison between LDA+DMFT(NCA) calculated parameters for both  $\alpha$  and  $\gamma$  phases at  $T = 580$  K and experimental values.

	$\alpha$ -Ce LDA+DMFT(NCA)	$\alpha$ -Ce [3]	$\alpha$ -Ce [20]	$\gamma$ -Ce LDA+DMFT(NCA)	$\gamma$ -Ce [3]	$\gamma$ -Ce [20]
$P_0$	0.126	0.1558		0.0150	0.0426	
$P_1$	0.829	0.8079		0.9426	0.9444	
$P_2$	0.044	0.0264		0.0423	0.0131	
$n_f$	0.908	0.861	0.8	1.014	0.971	1
$T_K$ , [K]	1000	945	1800,2000	30	95	60
$\chi(0)$ , [ $10^{-3}emu/mol$ ]	1.08	0.70	0.53	24	8.0	12
$\Delta_{av}$ , [meV]	86.6	66.3		42.7	32.2	